Accepted Manuscript

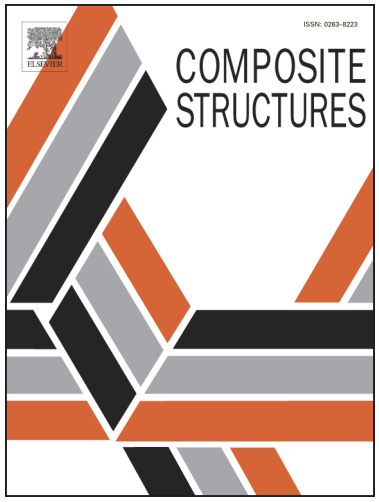

Vibration and nonlinear dynamic response of imperfect three-phase polymer nanocomposite panel resting on elastic foundations under hydrodynamic loads

Nguyen Dinh Duc, Homayoun Hadavinia, Pham Van Thu, Tran Quoc Quan

PII: S0263-8223(15)00369-4
DOI: http://dx.doi.org/10.1016/j.compstruct.2015.05.009
Reference: COST 6422

To appear in: *Composite Structures*

Please cite this article as: Duc, N.D., Hadavinia, H., Thu, P.V., Quan, T.Q., Vibration and nonlinear dynamic response of imperfect three-phase polymer nanocomposite panel resting on elastic foundations under hydrodynamic loads, *Composite Structures* (2015), doi: http://dx.doi.org/10.1016/j.compstruct.2015.05.009

Vibration and nonlinear dynamic response of imperfect three-phase polymer nanocomposite panel resting on elastic foundations under hydrodynamic loads

Nguyen Dinh Duc[1]*, Homayoun Hadavinia[2], Pham Van Thu[3], Tran Quoc Quan[1]

[1]*Vietnam National University, Hanoi -144 Xuan Thuy - Cau Giay - Hanoi – Vietnam*
[2]*School of Mechanical & Automotive Engineering, Kingston University London, UK*
[3]*Nha Trang University, Vietnam*

Abstract: An investigation on the nonlinear dynamic response and vibration of the imperfect laminated three-phase polymer nanocomposite panel resting on elastic foundations and subjected to hydrodynamic loads is presented in this paper. The formulations are based on the classical shell theory and stress function taking into account geometrical nonlinearity, initial geometrical imperfection and Pasternak type elastic foundation. Numerical results for dynamic response and vibration of the three-phase polymer composite panel are obtained by Runge-Kutta method. The influences of fibers and particles, material and geometrical properties, foundation stiffness, imperfection and hydrodynamic loads on the nonlinear dynamic response and nonlinear vibration of the three-phase composite panel are discussed in detail.

Keywords: Nonlinear dynamic, vibration, laminated three-phase polymer nanocomposite panel, hydrodynamics loads, imperfection, elastic foundations.

1. Introduction

Currently, composite materials have become indispensable in several applications, such as high-performance structures in many fields of civil, marine and aerospace engineering, among others. The mechanical behaviors of composite structures, such as bending, vibration, stability, buckling, etc., has attracted attention of many researchers. Rango et al. [1] presented the formulation of an enriched macro element suitable to analyze the free vibration response of composite plate assemblies. Bodaghi et al. [2] investigated thermo-mechanical analysis of rectangular shape adaptive composite plates with surface bonded shape memory alloy ribbons. Sahoo and Singh [3] used a new trigonometric zigzag theory to research the analysis of laminated composite and

* Corresponding author: Email: ducnd@vnu.edu.vn (Duc ND)

sandwich plates. Samadpour et al. [4] studied nonlinear free vibration of thermally buckled sandwich plate with embedded pre-strained shape memory alloy fibers in temperature dependent laminated composite face sheets. Moleiro et al. [5] provided an assessment of layerwise mixed models using least-squares formulation for the coupled electromechanical static analysis of multilayered plates. Heydarpour et al. [6] examined the influences of centrifugal and Coriolis forces on the free vibration behavior of rotating carbon nanotube reinforced composite truncated conical shells. Lopatin and Morozov [7] considered free vibrations of a cantilever composite circular cylindrical shell. Burgueño et al. [8] presented approaches for modifying and controlling the elastic response of axially compressed laminated composite cylindrical shells in the far postbuckling regime. The vibration and damping characteristics of free–free composite sandwich cylindrical shell with pyramidal truss-like cores have been conducted by Yang et al. [9] using the Rayleigh–Ritz model and finite element method.

Three-phase composite is a material consisted of matrix, the reinforced fibers and particles which have been investigated by Vanin and Duc [10]. Shen et al. [11] analyzed a coated inclusion of arbitrary shape embedded in a three-phase composite plate subjected to anti-plane mechanical and in-plane electrical loadings. Lin et al. [12] presented a solution of magnetoelastic stresses on a three-phase composite cylinder subjected to a remote uniform magnetic induction. Wu et al. [13] developed an effective model to bound the effective magnetic permeability of three-phase composites with coated spherical inclusions. There are several claims on the deflection and the creep for the three-phase composite laminates in the bending state [14]. These findings have shown that optimal three-phase composite can be obtained by controlling the volume ratios of fiber and particles. Afonso et al. [15] introduced a new general model to calculate the elastic properties of three-phase composites by means of closed-form analytical solutions is presented. Andrianov et al. [16] analyzed the three-phase composite model from the viewpoint of the asymptotic homogenization method. Recently, Duc et al. [17,18] studied nonlinear stability of the three-phase polymer composite plate under thermal and mechanical loads.

This paper presents an investigation on the nonlinear dynamic response and vibration of the imperfect laminated three-phase polymer nanocomposite panels resting on elastic foundations and subjected to hydrodynamic loads. These structures have similar shape with the hydrofoil currently under investigation and manufacturing in Vietnam. The formulations are based on the classical shell theory and stress function taking into account geometrical nonlinearity, initial geometrical imperfection and Pasternak type elastic foundation. Numerical results for dynamic response and vibration of the three-phase polymer composite panel are obtained by Runge-Kutta method.

It is noted that the present paper is improvement and supplement of the ideas in proceeding paper which we presented at the Third International Conference on Engineering Mechanics and Automation [22] (ICEMA 3-2014, Hanoi, October- 2014), including SEM structures images of two-phase 2D composite (glass fibers, polymer matrix) and the three-phase 2Dm composite (glass fibers, titanium oxide particles and polymer matrix) in order to improve the paper more convinced.

2. Determination of the elastic modules of three-phase composite

In this paper, the algorithm which is successfully applied in Ref. [17,18] to determine the elastic modules of three-phase composite has been used. According to this algorithm, the elastic modules of 3-phase composites are estimated using two theoretical models of the 2-phase composite consecutively: $nD_m = O_m + nD$ [17,18]. This paper considers 3-phase composite reinforced with particles and unidirectional fibers, so the problem's model will be : $1D_m=O_m +1D$. Firstly, the modules of the effective matrix O_m which is called "effective modules" are calculated. In this step, the effective matrix consists of the original matrix and added particles. It is considered to be homogeneous, isotropic and have two elastic modules. The next step is estimating the elastic modules for a composite material consists of the effective matrix and unidirectional reinforced fibers.

Assuming that all the component phases (matrix, fiber and particles) are homogeneous and isotropic, we will use $E_m, E_a, E_c; \nu_m, \nu_a, \nu_c; \psi_m, \psi_a, \psi_c$ to denote Young's modulus and Poisson ratio and volume fraction for the matrix, fiber and particles,

respectively. Following [17,18], the modules for the effective composite can be obtained as below

$$\bar{G} = G_m \frac{1-\psi_c(7-5\nu_m)H}{1+\psi_c(8-10\nu_m)H}, \tag{1}$$

$$\bar{K} = K_m \frac{1+4\psi_c G_m L(3K_m)^{-1}}{1-4\psi_c G_m L(3K_m)^{-1}}, \tag{2}$$

where

$$L = \frac{K_c - K_m}{K_c + \frac{4G_m}{3}}, H = \frac{G_m/G_c - 1}{8-10\nu_m + (7-5\nu_m)\frac{G_m}{G_c}}. \tag{3}$$

$\bar{E}, \bar{\nu}$ can be calculate from ($\bar{G}, \bar{K}$) as below

$$\bar{E} = \frac{9\bar{K}\bar{G}}{3\bar{K}+\bar{G}}, \bar{\nu} = \frac{3\bar{K}-2\bar{G}}{6\bar{K}-2\bar{G}}. \tag{4}$$

The elastic moduli for three-phase composite reinforced with unidirectional fiber are chosen to be calculated using Vanin's formulas [20]

$$E_{11} = \psi_a E_a + (1-\psi_a)\bar{E} + \frac{8\bar{G}\psi_a(1-\psi_a)(\nu_a - \bar{\nu})}{2-\psi_a + \bar{x}\psi_a + (1-\psi_a)(x_a-1)\frac{\bar{G}}{G_a}},$$

$$E_{22} = \left\{ \frac{\nu_{21}^2}{E_{11}} + \frac{1}{8\bar{G}} \left[\frac{2(1-\psi_a)(\bar{\chi}-1) + (\chi_a-1)(\bar{\chi}-1+2\psi_a)\frac{\bar{G}}{G_a}}{2-\psi_a+\bar{\chi}\psi_a+(1-\psi_a)(\chi_a-1)\frac{\bar{G}}{G_a}} + 2\frac{\bar{\chi}(1-\psi_a)+(1+\psi_a\bar{\chi})\frac{\bar{G}}{G_a}}{\bar{\chi}+\psi_a+(1-\psi_a)\frac{\bar{G}}{G_a}} \right] \right\}^{-1},$$

$$G_{12} = \bar{G}\frac{1+\psi_a+(1-\psi_a)\frac{\bar{G}}{G_a}}{1-\psi_a+(1+\psi_a)\frac{\bar{G}}{G_a}}, G_{23} = \bar{G}\frac{\bar{\chi}+\psi_a+(1-\psi_a)\frac{\bar{G}}{G_a}}{(1-\psi_a)\bar{\chi}+(1+\bar{\chi}\psi_a)\frac{\bar{G}}{G_a}},$$

$$\frac{\nu_{23}}{E_{22}} = -\frac{\nu_{21}^2}{E_{11}} + \frac{1}{8\bar{G}} \left[2\frac{(1-\psi_a)\bar{x}+(1+\psi_a\bar{x})\frac{\bar{G}}{G_a}}{\bar{x}+\psi_a+(1-\psi_a)\frac{\bar{G}}{G_a}} - \frac{2(1-\psi_a)(\bar{x}-1)+(x_a-1)(\bar{x}-1+2\psi_a)\frac{\bar{G}}{G_a}}{2-\psi_a+\bar{x}\psi_a+(1-\psi_a)(x_a-1)\frac{\bar{G}}{G_a}} \right],$$

$$\nu_{21} = \bar{\nu} - \frac{(\bar{\chi}+1)(\bar{\nu}-\nu_a)\psi_a}{2-\psi_a+\bar{\chi}\psi_a+(1-\psi_a)(\chi_a-1)\frac{\bar{G}}{G_a}}, \tag{5}$$

in which

$$\overline{\chi} = 3 - 4\overline{\nu}, \overline{\chi_a} = 3 - 4\overline{\nu_a}. \quad (6)$$

To verify the validity of these equations, three-phase composite polymer made of polyester AKAVINA (made in Vietnam), glass fibers (made in Korea) and titanium oxide (made in Australia) with the properties shown in Table 1 was investigated [17,18].

Table 1

Properties of the component phases for three-phase composite

Component phase	**Young modulus E**	**Poisson ratio ν**
Matrix polyester AKAVINA (Vietnam)	1,43 GPa	0.345
Glass fiber (Korea)	22 GPa	0.24
Titanium oxide TiO_2 (Australia)	5,58 GPa	0.20

By using the SEM instrumentation at the Laboratory for Micro-Nano Technology, University of Engineering and Technology, Vietnam National University, Hanoi, Figs. 1 and 2 show the images of fabricated samples of composite structures which are made in the Institute of Ship building, Nha Trang University. Fig. 1 illustrates a SEM image of 2Dm composite polymer two-phase material (glass fibers volume fraction of 25% without particles) and Fig. 2 shows a SEM image of 2Dm composite polymer three-phase material (glass fibers volume fraction of 25% and Titanium oxide particles volume fraction of 3%). Obviously, when the particles are doped, the air cavities significantly reduced and the material is finer. In other words, particles enhance the stiffness and the penetration resistance of the materials.

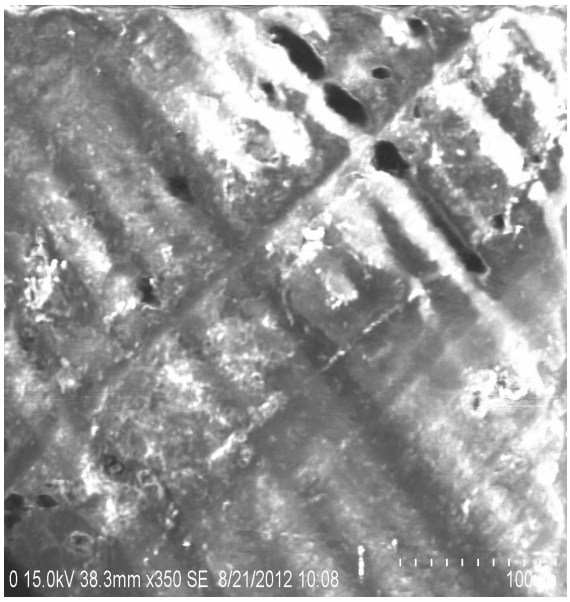

Fig 1. SEM image of 2Dm composite two-phase material (fibers volume fraction is 25% without particles).

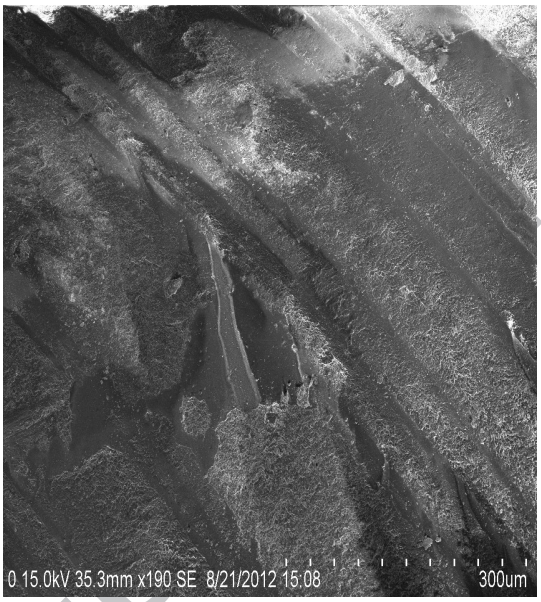

Fig. 2. SEM image of 2Dm composite three-phase material (fibers volume fraction is 25% and particles volume fraction is 3%).

3. Governing equations

Consider a three-phase composite panel subjected to hydrodynamic loads: hydrodynamic lift q_1 and drag q_2 as shown in Fig. 3. The panel is referred to a Cartesian coordinate system x, y, z, where xy is the mid-plane of the panel and z is the thickness coordinator, $-h/2 \le z \le h/2$. The radii of curvatures, length, width and total thickness of the panel are R, a, b and h, respectively.

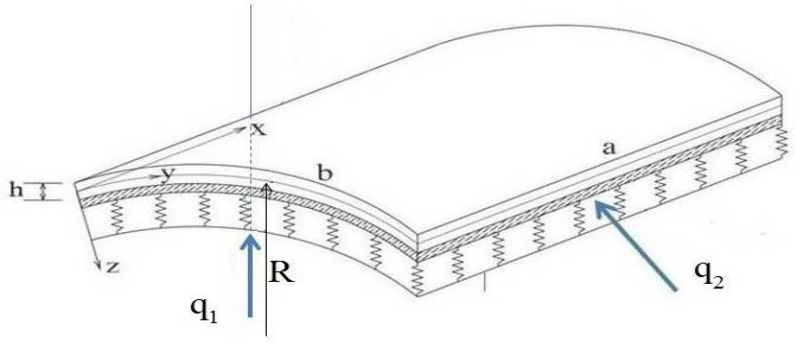

Fig. 3. Geometry and coordinate system of three-phase composite panels on elastic foundations.

In this study, we assumed that the panel is thin, so the classical laminated shell theory (CLST) is used to establish governing equations and determine the nonlinear response of composite panels. In the case of thick panel, we must use higher-order shear deformation theories. By choosing of accurate theories can refer to [23].

Taking into account the von Karman nonlinearity, the strain-displacement relations are

$$\begin{pmatrix} \varepsilon_x \\ \varepsilon_y \\ \gamma_{xy} \end{pmatrix} = \begin{pmatrix} \varepsilon_x^0 \\ \varepsilon_y^0 \\ \gamma_{xy}^0 \end{pmatrix} + z \begin{pmatrix} k_x \\ k_y \\ k_{xy} \end{pmatrix}, \tag{7}$$

where

$$\begin{pmatrix} \varepsilon_x^0 \\ \varepsilon_y^0 \\ \gamma_{xy}^0 \end{pmatrix} = \begin{pmatrix} u_{,x} + w_{,x}^2 / 2 \\ v_{,y} - w / R + w_{,y}^2 / 2 \\ u_{,y} + v_{,x} + w_{,x} w_{,y} \end{pmatrix}, \begin{pmatrix} k_x \\ k_y \\ k_{xy} \end{pmatrix} = \begin{pmatrix} -w_{,xx} \\ -w_{,yy} \\ -2w_{,xy} \end{pmatrix}, \tag{8}$$

in which u, v are the displacement components along the x, y directions, respectively.

Hooke law for a laminated composite panel is defined as

$$\begin{pmatrix} \sigma_x \\ \sigma_y \\ \sigma_{xy} \end{pmatrix}_k = \begin{pmatrix} Q_{11}^{'} & Q_{12}^{'} & Q_{16}^{'} \\ Q_{12}^{'} & Q_{22}^{'} & Q_{26}^{'} \\ Q_{16}^{'} & Q_{26}^{'} & Q_{66}^{'} \end{pmatrix}_k \begin{pmatrix} \varepsilon_x \\ \varepsilon_y \\ \gamma_{xy} \end{pmatrix}_k, \tag{9}$$

in which k is the number of layers and

$$\begin{aligned}
Q_{11}^{'} &= Q_{11}\cos^4\theta + Q_{22}\sin^4\theta + 2(Q_{12} + 2Q_{66})\sin^2\theta\cos^2\theta, \\
Q_{12}^{'} &= Q_{12}(\cos^4\theta + \sin^4\theta) + (Q_{11} + Q_{22} - 4Q_{66})\sin^2\theta\cos^2\theta, \\
Q_{12}^{'} &= Q_{12}(\cos^4\theta + \sin^4\theta) + (Q_{11} + Q_{22} - 4Q_{66})\sin^2\theta\cos^2\theta, \\
Q_{16}^{'} &= (Q_{12} - Q_{22} + 2Q_{66})\sin^3\theta\cos\theta + (Q_{11} - Q_{12} - 2Q_{66})\sin\theta\cos^3\theta, \\
Q_{22}^{'} &= Q_{11}\sin^4\theta + Q_{22}\cos^4\theta + 2(Q_{12} + 2Q_{66})\sin^2\theta\cos^2\theta, \\
Q_{26}^{'} &= (Q_{11} - Q_{12} - 2Q_{66})\sin^3\theta\cos\theta + (Q_{12} - Q_{22} + 2Q_{66})\sin\theta\cos^3\theta, \\
Q_{66}^{'} &= Q_{66}(\sin^4\theta + \cos^4\theta) + \left[Q_{11} + Q_{22} - 2(Q_{12} + Q_{66})\right]\sin^2\theta\cos^2\theta,
\end{aligned} \tag{10}$$

and

$$Q_{11}=\frac{E_{11}}{1-\frac{E_{22}}{E_{11}}\nu_{12}^2}=\frac{E_{11}}{1-\nu_{12}\nu_{21}},Q_{22}=\frac{E_{22}}{1-\frac{E_{22}}{E_{11}}\nu_{12}^2}=\frac{E_{22}}{E_{11}}Q_{11},$$
$$Q_{12}=\frac{E_{11}}{1-\frac{E_{22}}{E_{11}}\nu_{12}^2}=\frac{\nu_{12}}{Q_{22}},Q_{66}=G_{12}, \tag{11}$$

where θ is the angle between the fiber direction and the coordinate system. The force and moment resultants of the laminated composite panels are determined by

$$N_i=\sum_{k=1}^{n}\int_{h_{k-1}}^{h_k}[\sigma_i]_k\,dz,\ i=x,y,xy,$$
$$M_i=\sum_{k=1}^{n}\int_{h_{k-1}}^{h_k}z[\sigma_i]_k\,dz,\ i=x,y,xy. \tag{12}$$

Substitution of Eq. (7) into Eq. (9) and the result into Eq. (12) give the constitutive relations as

$$\begin{aligned}&(N_x,N_y,N_{xy})=(A_{11},A_{12},A_{16})\varepsilon_x^0+(A_{12},A_{22},A_{26})\varepsilon_y^0+(A_{16},A_{26},A_{66})\gamma_{xy}^0\\&+(B_{11},B_{12},B_{16})k_x+(B_{12},B_{22},B_{26})k_y+(B_{16},B_{26},B_{66})k_{xy},\\&(M_x,M_y,M_{xy})=(B_{11},B_{12},B_{16})\varepsilon_x^0+(B_{12},B_{22},B_{26})\varepsilon_y^0+(B_{16},B_{26},B_{66})\gamma_{xy}^0\\&+(D_{11},D_{12},D_{16})k_x+(D_{12},D_{22},D_{26})k_y+(D_{16},D_{26},D_{66})k_{xy},\end{aligned} \tag{13}$$

where

$$A_{ij}=\sum_{k=1}^{n}(Q_{ij}^{'})_k(h_k-h_{k-1}),\ i,j=1,2,6,$$
$$B_{ij}=\frac{1}{2}\sum_{k=1}^{n}(Q_{ij}^{'})_k(h_k^2-h_{k-1}^2)\ i,j=1,2,6, \tag{14}$$
$$D_{ij}=\frac{1}{3}\sum_{k=1}^{n}(Q_{ij}^{'})_k(h_k^3-h_{k-1}^3)\ i,j=1,2,6.$$

The nonlinear motion equation of the composite panels based on CLST with the Volmir's assumption [19], $u<<w,v<<w,\rho_1\frac{\partial^2 u}{\partial t^2}\to 0,\ \rho_1\frac{\partial^2 v}{\partial t^2}\to 0$ are given by

$$N_{x,x}+N_{xy,y}=0 \tag{15a}$$
$$N_{xy,x}+N_{y,y}=0 \tag{15b}$$

$$M_{x,xx} + 2M_{xy,xy} + M_{y,yy} + N_x w_{,xx} + 2N_{xy} w_{,xy} + N_y w_{,yy} + q_1 + q_2 - k_1 \mathrm{w}$$
$$+k_2 \nabla^2 \mathrm{w} + \frac{N_y}{R} = \rho_1 \frac{\partial^2 \mathrm{w}}{\partial t^2} \tag{15c}$$

where $\rho_1 = \rho h$ with ρ is the mass density of composite panels and q_1, q_2 are hydrodynamic lift and drag forces which are experimentally determined and they depend on the velocities according to the Matveev's formulas. These forces for the ship with length of 16.4 m, width of 3.4 m and volume of occupied water 12000 kg are tabulated in Table 2 [21].

Table 2

The dependency of hydrodynamic lift and drag on the velocities

Velocity (m/s)	Lift (N)	Drag (N)
10	110537	5550.8
10.2	112730	5380.6
10.4	114204	5165.6
10.6	117836	5243.2
10.9	121090	5130.6
12	129529	4416.1

Calculated from Eq. (13)

$$\begin{aligned}
\varepsilon_x^0 &= A_{11}^* N_x + A_{12}^* N_y + A_{16}^* N_{xy} - B_{11}^* k_x - B_{12}^* k_y - B_{16}^* k_{xy}, \\
\varepsilon_y^0 &= A_{12}^* N_x + A_{22}^* N_y + A_{26}^* N_{xy} - B_{21}^* k_x - B_{22}^* k_y - B_{26}^* k_{xy}, \\
\varepsilon_{xy}^0 &= A_{16}^* N_x + A_{26}^* N_y + A_{66}^* N_{xy} - B_{16}^* k_x - B_{26}^* k_y - B_{66}^* k_{xy},
\end{aligned} \tag{16}$$

where

$$A_{11}^{*}=\frac{A_{22}A_{66}-A_{26}^{2}}{\Delta},A_{12}^{*}=\frac{A_{16}A_{26}-A_{12}A_{66}}{\Delta},A_{16}^{*}=\frac{A_{12}A_{26}-A_{22}A_{16}}{\Delta},$$
$$A_{22}^{*}=\frac{A_{11}A_{66}-A_{16}^{2}}{\Delta},A_{26}^{*}=\frac{A_{12}A_{16}-A_{11}A_{26}}{\Delta},A_{66}^{*}=\frac{A_{11}A_{22}-A_{12}^{2}}{\Delta},$$
$$A_{22}^{*}=\frac{A_{11}A_{66}-A_{16}^{2}}{\Delta},A_{26}^{*}=\frac{A_{12}A_{16}-A_{11}A_{26}}{\Delta},A_{66}^{*}=\frac{A_{11}A_{22}-A_{12}^{2}}{\Delta},$$
$$\Delta=A_{11}A_{22}A_{66}-A_{11}A_{26}^{2}+2A_{12}A_{16}A_{26}-A_{12}^{2}A_{66}-A_{16}^{2}A_{22},$$
$$B_{11}^{*}=A_{11}^{*}B_{11}+A_{12}^{*}B_{12}+A_{16}^{*}B_{16},B_{12}^{*}=A_{11}^{*}B_{12}+A_{12}^{*}B_{22}+A_{16}^{*}B_{26},\quad(17)$$
$$B_{16}^{*}=A_{11}^{*}B_{16}+A_{12}^{*}B_{26}+A_{16}^{*}B_{66},B_{21}^{*}=A_{12}^{*}B_{11}+A_{22}^{*}B_{12}+A_{26}^{*}B_{16},$$
$$B_{22}^{*}=A_{12}^{*}B_{12}+A_{22}^{*}B_{22}+A_{26}^{*}B_{26},B_{26}^{*}=A_{12}^{*}B_{16}+A_{22}^{*}B_{26}+A_{26}^{*}B_{66},$$
$$B_{61}^{*}=A_{16}^{*}B_{11}+A_{26}^{*}B_{12}+A_{66}^{*}B_{16},B_{62}^{*}=A_{16}^{*}B_{12}+A_{26}^{*}B_{22}+A_{66}^{*}B_{26},$$
$$B_{66}^{*}=A_{16}^{*}B_{16}+A_{26}^{*}B_{26}+A_{66}^{*}B_{66}.$$

Substituting once again Eq. (16) into the expression of M_{ij} in (13), then M_{ij} into the Eq. (15c) leads to

$$N_{x,x}+N_{xy,y}=0,$$
$$N_{xy,x}+N_{y,y}=0,$$
$$P_1f_{,xxxx}+P_2f_{,yyyy}+P_3w_{,xxyy}+P_4w_{,xxxy}+P_5w_{,xyyy}+P_6w_{,xxxx}+P_7w_{,yyyy}+P_8w_{,xxyy}$$
$$+P_9w_{,xxxy}+P_{10}w_{,xyyy}+N_xw_{,xx}+2N_{xy}w_{,xy}+N_yw_{,yy}+q_1+q_2-k_1\mathrm{w}+k_2\nabla^2\mathrm{w}+\frac{N_y}{R}=\rho_1\frac{\partial^2\mathrm{w}}{\partial t^2},\quad(18)$$

where

$$P_1=B_{21}^{*},P_2=B_{12}^{*},P_3=B_{11}^{*}+B_{22}^{*}-2B_{66}^{*},P_4=2B_{26}^{*}-B_{61}^{*},$$
$$P_5=2B_{16}^{*}-B_{62}^{*},P_6=B_{11}B_{11}^{*}+B_{12}B_{21}^{*}+B_{16}B_{61}^{*},P_7=B_{12}B_{12}^{*}+B_{22}B_{22}^{*}+B_{26}B_{62}^{*},$$
$$P_8=B_{11}B_{12}^{*}+B_{12}B_{22}^{*}+B_{16}B_{62}^{*}+B_{12}B_{11}^{*}+B_{22}B_{21}^{*}+B_{26}B_{61}^{*}+4B_{16}B_{16}^{*}+4B_{26}B_{26}^{*}+4B_{66}B_{66}^{*},\quad(19)$$
$$P_9=2(B_{11}B_{16}^{*}+B_{12}B_{26}^{*}+B_{16}B_{66}^{*}+B_{16}B_{11}^{*}+B_{26}B_{21}^{*}+B_{66}B_{61}^{*}),$$
$$P_{10}=2(B_{12}B_{16}^{*}+B_{22}B_{26}^{*}+B_{26}B_{66}^{*}+B_{16}B_{12}^{*}+B_{26}B_{22}^{*}+B_{66}B_{62}^{*}).$$

$f(x,y)$ is stress function defined by

$$N_x=f_{,yy},\ N_y=f_{,xx},\ N_{xy}=-f_{,xy}\quad(20)$$

For an imperfect laminated composite panel, Eq. (18) are modified to

$$P_1f_{,xxxx}+P_2f_{,yyyy}+P_3w_{,xxyy}+P_4w_{,xxxy}+P_5w_{,xyyy}+P_6w_{,xxxx}+P_7w_{,yyyy}+P_8w_{,xxyy}$$
$$+P_9w_{,xxxy}++P_{10}w_{,xyyy}+f_{,yy}\left(w_{,xx}+w_{,xx}^{*}\right)-2f_{,xy}\left(w_{,xy}+w_{,xy}^{*}\right)+f_{,xx}\left(w_{,yy}+w_{,yy}^{*}\right)\quad(21)$$
$$+q_1+q_2-k_1\mathrm{w}+k_2\nabla^2\mathrm{w}+\frac{N_y}{R}=\rho_1\frac{\partial^2\mathrm{w}}{\partial t^2},$$

in which $w^*(x,y)$ is a known function representing initial small imperfection of the panel.

The geometrical compatibility equation for an imperfect composite panel is written as

$$\varepsilon^0_{x,yy}+\varepsilon^0_{y,xx}-\gamma^0_{xy,xy}=w^2_{,xy}-w_{,xx}w_{,yy}+2w_{,xy}w^*_{,xy}-w_{,xx}w^*_{,yy}-w_{,yy}w^*_{,xx}-\frac{w_{,xx}}{R}. \tag{22}$$

From the constitutive relations (16) in conjunction with Eq. (20) one can write

$$\begin{aligned}
\varepsilon^0_x &= A^*_{11}f_{,yy}+A^*_{12}f_{,xx}-A^*_{16}f_{,xy}-B^*_{11}k_x-B^*_{12}k_y-B^*_{16}k_{xy},\\
\varepsilon^0_y &= A^*_{12}f_{,yy}+A^*_{22}f_{,xx}-A^*_{26}f_{,xy}-B^*_{21}k_x-B^*_{22}k_y-B^*_{26}k_{xy},\\
\varepsilon^0_{xy} &= A^*_{16}f_{,yy}+A^*_{26}f_{,xx}-A^*_{66}f_{,xy}-B^*_{16}k_x-B^*_{26}k_y-B^*_{66}k_{xy},
\end{aligned} \tag{23}$$

Setting Eq. (23) into Eq. (22) gives the compatibility equation of an imperfect composite panel as

$$\begin{aligned}
&A^*_{22}f_{,xxxx}+E_1f_{,xxyy}+A^*_{11}f_{,yyyy}-2A^*_{26}f_{,xxxy}-2A^*_{16}f_{,xyyy}+B^*_{21}\mathrm{w}_{,xxxx}+B^*_{12}\mathrm{w}_{,yyyy}\\
&+E_2\mathrm{w}_{,xxyy}+E_3\mathrm{w}_{,xxxy}+E_4\mathrm{w}_{,xyyy}-\begin{pmatrix} w^2_{,xy}-w_{,xx}w_{,yy}+2w_{,xy}w^*_{,xy}\\ -w_{,xx}w^*_{,yy}-w_{,yy}w^*_{,xx}-\dfrac{w_{,xx}}{R}\end{pmatrix}=0,
\end{aligned} \tag{24}$$

where

$$\begin{aligned}
&E_1=2A^*_{12}+A^*_{66}, E_2=B^*_{11}+B^*_{22}-2B^*_{66},\\
&E_3=2B^*_{26}-B^*_{61}, E_4=2B^*_{16}+B^*_{62}.
\end{aligned} \tag{25}$$

Eqs. (21) and (24) are nonlinear equations in terms of variables w and f and they can be used to investigate the stability of thin composite panels on elastic foundations subjected to hydrodynamic loads.

4. Nonlinear dynamical analysis

A three-phase composite panel considered in this paper is assumed to be simply supported and subjected to lift q_1, drag q_2 forces and axial compression of intensities P_x and P_y respectively at its cross section. Thus the boundary conditions are

$$\begin{aligned}
&w=N_{xy}=M_x=0,\ N_x=-P_xh \text{ at } x=0,a,\\
&w=N_{xy}=M_y=0,\ N_y=-P_yh \text{ at } y=0,b.
\end{aligned} \tag{26}$$

The approximate solutions of w, w^* and f satisfying boundary condition (26) are assumed to be [17,18]

$$\left(w, w^*\right) = \left(W, \mu h\right) \sin \lambda_m x \sin \delta_n y, \tag{27a}$$

$$f = A_1 \cos 2\lambda_m x + A_2 \cos 2\delta_n y + A_3 \sin \lambda_m x \sin \delta_n y + A_4 \cos \lambda_m x \cos \delta_n y + \frac{1}{2} N_{x0} y^2 + \frac{1}{2} N_{y0} x^2, \tag{27b}$$

$\lambda_m = m\pi / a$, $\delta_n = n\pi / b$, W is amplitude of the deflection and μ is imperfection parameter. The coefficients A_i $(i = 1 \div 4)$ are determined by substitution of Eqs. (27a), (27b) into Eq. (24) as

$$\begin{aligned} A_1 &= \frac{1}{32 A_{22}^*} \frac{\delta_n^2}{\lambda_m^2} W(W + 2\mu h), A_2 = \frac{1}{32 A_{11}^*} \frac{\lambda_m^2}{\delta_n^2} W(W + 2\mu h), \\ A_3 &= \frac{(F_2 F_4 - F_1 F_3)}{F_2^2 - F_1^2} W, A_4 = \frac{(F_2 F_3 - F_1 F_4)}{F_2^2 - F_1^2} W, \end{aligned} \tag{28}$$

where $F_i (i = 1 \div 4)$ are given in Appendix A.

Subsequently, substitution of Eqs. (27a), (27b) into Eq. (21) and applying the Galerkin procedure for the resulting equation yield

$$\begin{aligned} &\frac{ab}{4}[P_1 \frac{(F_2 F_4 - F_1 F_3)}{F_2^2 - F_1^2} \lambda_m^4 + P_2 \frac{(F_2 F_4 - F_1 F_3)}{F_2^2 - F_1^2} \delta_n^4 + P_3 \frac{(F_2 F_4 - F_1 F_3)}{F_2^2 - F_1^2} \lambda_m^2 \delta_n^2 - P_4 \frac{(F_2 F_3 - F_1 F_4)}{F_2^2 - F_1^2} \\ &- P_5 \frac{(F_2 F_3 - F_1 F_4)}{F_2^2 - F_1^2} + P_6 \lambda_m^4 + P_7 \delta_n^4 + P_8 \lambda_m^2 \delta_n^2 - \frac{(F_2 F_4 - F_1 F_3)}{F_2^2 - F_1^2} \frac{\lambda_m^2}{R} - k_1 - k_2 (\lambda_m^2 + \delta_n^2)] W \\ &- \left[\frac{2}{3} \lambda_m \delta_n \left(P_1 \frac{1}{A_{22}^*} + P_2 \frac{1}{A_{11}^*} \right) - \frac{1}{6RA_{22}^*} \frac{\delta_n}{\lambda_m} \right] W \left(W + 2\mu h\right) \\ &- \frac{ab}{64} \left(\frac{1}{A_{22}^*} \delta_n^4 + \frac{1}{A_{11}^*} \lambda_m^4 \right) W \left(W + \mu h\right)\left(W + 2\mu h\right) + \frac{8}{3} \frac{(F_2 F_4 - F_1 F_3)}{F_2^2 - F_1^2} \lambda_m \delta_n \mathrm{W} \left(W + \mu h\right) \\ &+ \frac{abh}{4} \left(P_x \lambda_m^2 + P_y \delta_n^2 \right)\left(W + \mu h\right) + \frac{4(q_1 + q_2)}{\lambda_m \delta_n} - \frac{4h}{\lambda_m \delta_n} \frac{P_y}{R} = \frac{ab\rho_1}{4} \frac{\partial^2 W}{\partial t^2}, \end{aligned} \tag{29}$$

where m, n are odd numbers. This basic equation is used to investigate the nonlinear dynamic response of three-phase polymer composite panels under hydrodynamic loads. The initial conditions are assumed as $W(0) = 0, \dot{W}(0) = 0$. The nonlinear equation (29) can be solved by the Runge-Kutta method.

From Eq. (29), the fundamental frequencies of a perfect panel can be determined approximately by an explicit expression

$$\omega_{mn} = \sqrt{-\frac{(b_1 + b_2)}{\rho_1}}, \tag{30}$$

where $b_i (i = 1,2)$ are given in Appendix A.

5. Results and Discussions

The results presented in this section from Eq. (29) correspond to deformation mode with half-wave numbers $m = n = 1$.

To determine the influences of fibers and particles, material and geometrical properties, foundation stiffness, imperfection and hydrodynamic loads on the nonlinear dynamic response of the three-phase composite panel, we consider the five-layers symmetric panel with stacking sequence of [45/-45/0/-45/45]. The mass density of the panel is $\rho = 1550 kg / m^3$.

Table 3 shows the effects of particles volume fraction, fiber volume fraction and elastic foundations on natural frequencies of the three-phase composite polymer panel. It can be seen that the value of the natural oscillation frequency increases when the values k_1 and k_2 increase. Furthermore, the Pasternak elastic foundation influences on the natural oscillation frequency larger than the Winkler foundation. The natural frequencies of the panels observed to be dependent on the particles volume fraction, fiber volume fraction, they decreases when increasing the particles volume fraction ψ_c and fiber volume fraction ψ_a and the effect of fiber to natural frequency is stronger than particle.

Table 3

Effects of particles volume fraction, fiber volume fraction and elastic foundations on natural frequencies of the three-phase composite polymer panel

ψ_a	ψ_c	$\omega_L (rad/s)$	
		$(k_1, k_2) = (0,0)$	$(k_1, k_2) = (0.01, 0.002)$
0.2	0	3.3258e3	4.8564e3
0.2	0.1	3.3038e3	4.8414e3

0.2	0.2	3.2981e3	4.8375e3
0.2	0.3	3.2763e3	4.8255e3
0	0.2	3.4884e3	5.1195e3
0.1	0.2	3.3975e3	4.9695e3
0.3	0.2	3.1015e3	4.7057e3

Figs. 4 and 5 represent the effect of the particles and the fibers volume fraction on dynamic response of three-phase polymer composite panel. We can realize that the increase of the particles and fibers density will decrease the amplitude of the panel. However, the effects of the fibers are stronger.

Figs. 6, 7 and 8 illustrate the effect of geometric factors b/a, b/h, R/h on nonlinear dynamic response of three-phase laminated polymer composite panel. From these figures, the amplitude of the panel increases when increasing the ratio b/a and decreasing the ratios b/h, R/h.

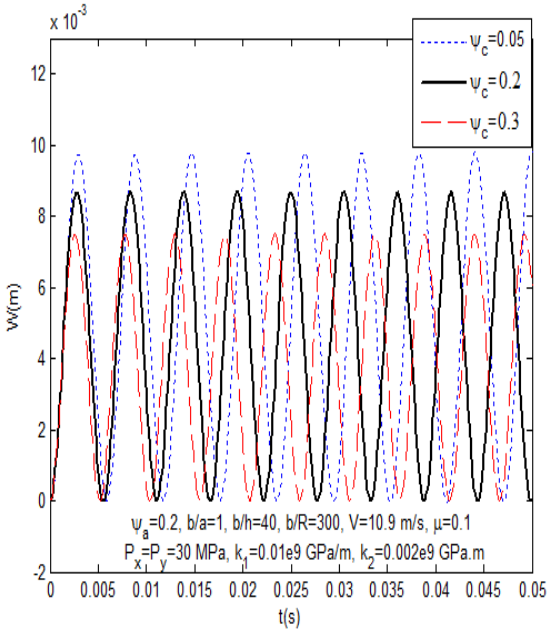

Fig. 4. Effects of particles volume fraction ψ_c on the dynamic response of three-phase polymer composite panel.

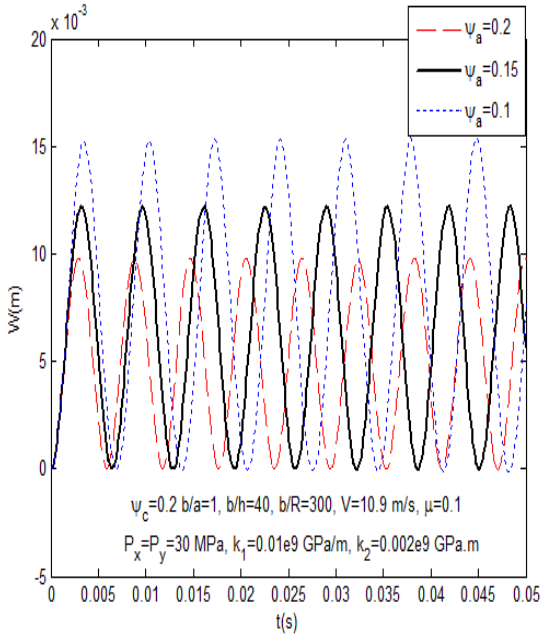

Fig. 5. Effects of fiber volume fraction ψ_a on the dynamic response of three-phase polymer composite panel.

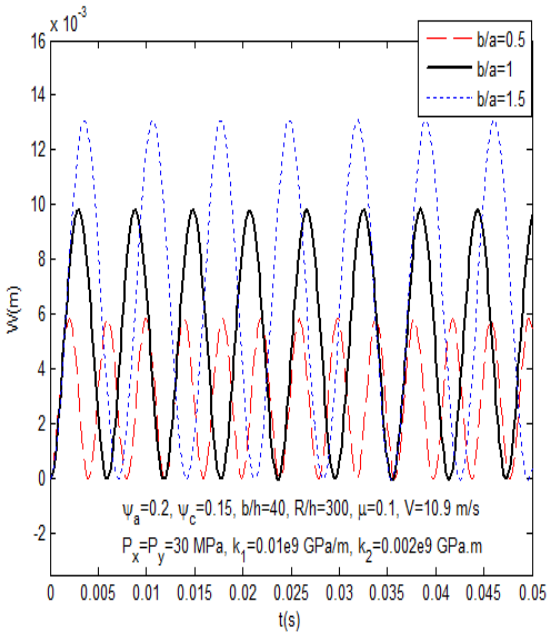

Fig. 6. Effect of b/a ratio on nonlinear dynamic response of three-phase polymer composite panel.

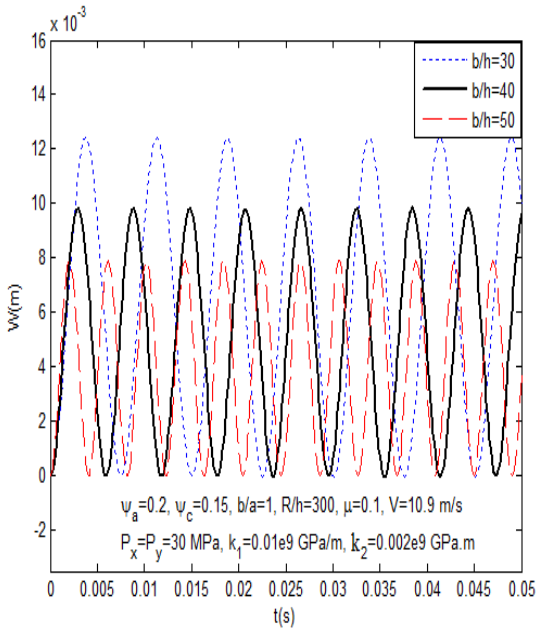

Fig. 7. Effect of b/h ratio on nonlinear dynamic response of three-phase polymer composite panel.

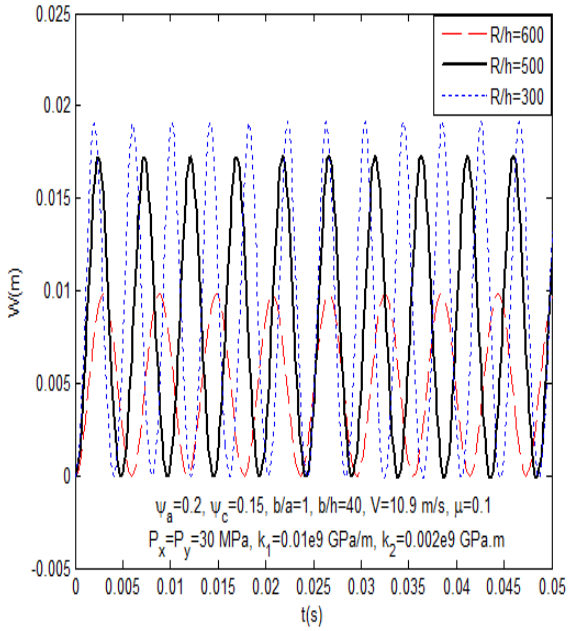

Fig. 8. Effect of R/h ratio on nonlinear dynamic response of three-phase polymer composite panel.

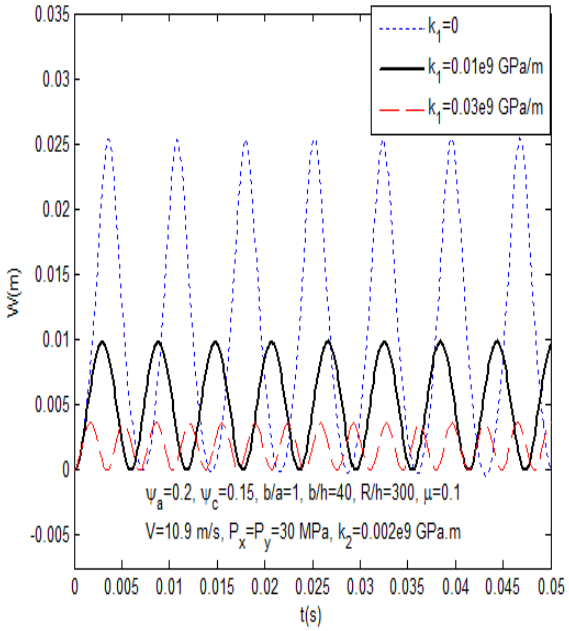

Fig. 9. Effect of the linear Winkler foundation on nonlinear dynamic response of three-phase polymer composite panel.

Figs. 9 and 10 show the effect of elastic foundation stiffness on the nonlinear dynamic response of three-phase polymer composite panel. It is clear that the panel fluctuation amplitude decreases when the stiffnesses k_1 and k_2 increase, namely, the amplitude of the panel decreases when it rests on elastic foundations, and the beneficial effect of the Pasternak foundation is better than the Winkler one.

Fig. 11 shows the effect of velocity on nonlinear dynamic response of three-phase polymer composite panel. It can be seen that the three-phase polymer composite panel fluctuation amplitudes increase when velocity increases. Fig. 12 shows the effect of pre-loaded axial compression P_y on the nonlinear dynamic response of the panel. This figure also indicates that the nonlinear dynamic response amplitude of the panel increases when the value of the pre-loaded axial compressive force P_y increases.

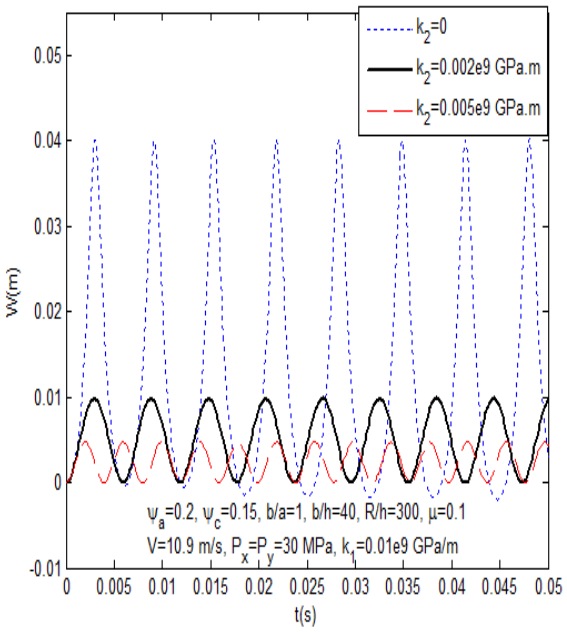

Fig. 10. Effect of the Pasternak foundation on nonlinear dynamic response of three-phase polymer composite panel.

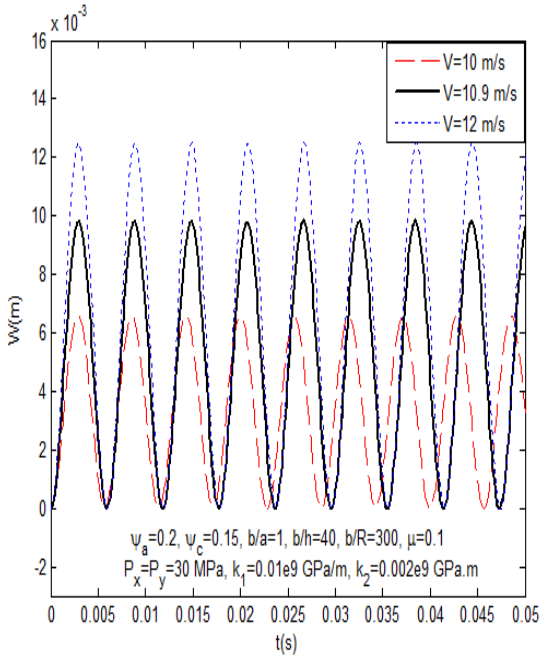

Fig. 11. Nonlinear dynamic responses of three-phase polymer composite panel with different velocities.

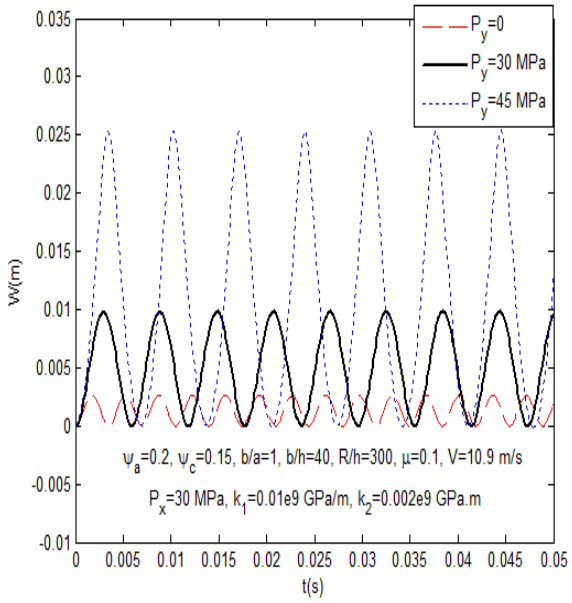

Fig. 12. Effect of pre-loaded axial compression P_y on nonlinear response of three-phase polymer composite panel.

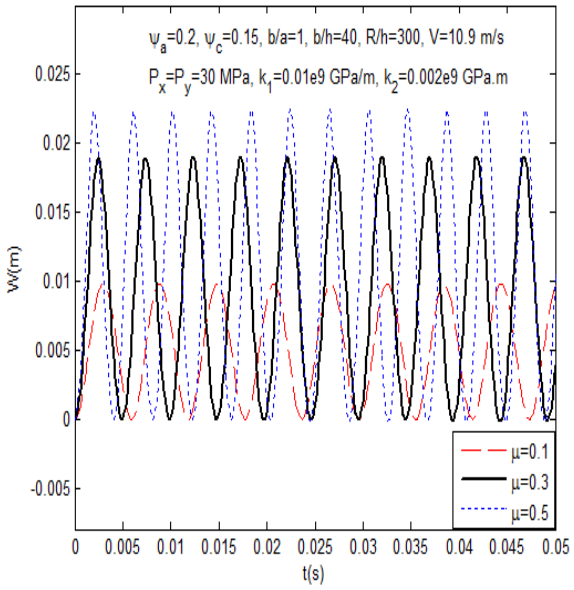

Fig. 13. Effect of imperfection parameter μ on nonlinear dynamic response of three-phase polymer composite panel.

Fig. 13 shows the effect of initial imperfection on the dynamic response of three-phase polymer composite panel. Obviously, the amplitude of the panel will increase and lose the stability if the initial imperfection increases.

Fig. 14 compares the nonlinear dynamic response of three-phase polymer composite panel in two cases: five-layers asymmetric panel with the stacking sequence of [0/45/45/-45/-45] and five-layers symmetric panel with the stacking sequence of [45/-45/0/-45/45]. This comparison is performed on panels with the same plies orientations and the same thickness. Clearly, the amplitude of asymmetric panel is higher than symmetric panel.

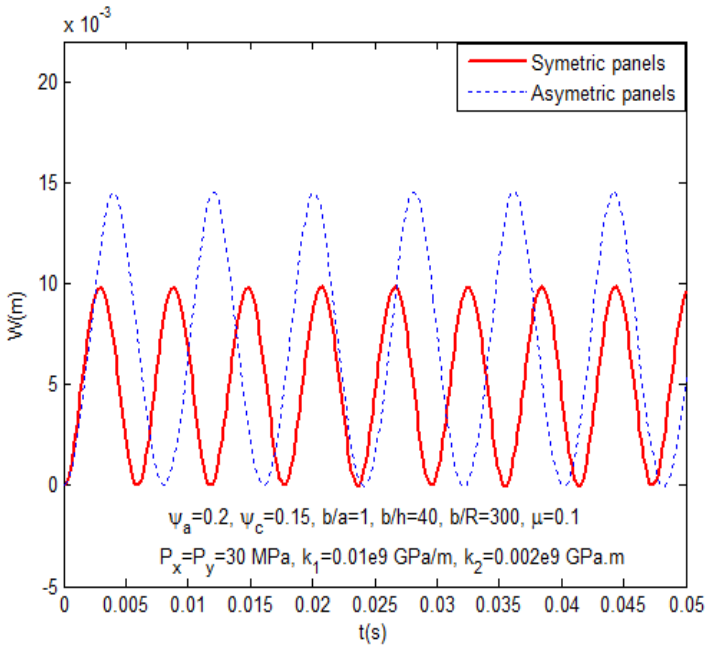

Fig. 14. Nonlinear dynamic response of three-phase polymer composite panel with different fiber angles.

6. Conclusions

This paper presented an analytical approach to investigate the nonlinear dynamic response and vibration of the imperfect laminated three-phase polymer nanocomposite panel resting on elastic foundations and subjected to hydrodynamic loads. The formulations are based on the classical laminated shell theory (CLST) and stress function taking into account geometrical nonlinearity, initial geometrical imperfection and Pasternak type elastic foundation. Numerical results for dynamic response and vibration of the three-phase polymer composite panel are obtained by Runge-Kutta method. The influence of fibers and particles volume fraction, material and geometrical properties, foundation stiffness, imperfection and hydrodynamic loads on the nonlinear dynamic response and nonlinear vibration of the three-phase composite panel are discussed in detail.

Appendix A

$$F_1 = A_{22}^* \lambda_m^4 + A_{11}^* \delta_n^4 + E_1 \lambda_m^2 \delta_n^2, F_2 = 2A_{26}^* \lambda_m^3 \delta_n + 2A_{16}^* \lambda_m \delta_n^3,$$

$$F_3 = \frac{\lambda_m^2}{R} - B_{21}^* \lambda_m^4 - B_{12}^* \delta_n^4 - E_2 \lambda_m^2 \delta_n^2, F_4 = E_3 \lambda_m^3 \delta_n + E_4 \lambda_m \delta_n^3,$$

$$b_1 = P_1\frac{(F_2F_4 - F_1F_3)}{F_2^2 - F_1^2}\lambda_m^4 + P_2\frac{(F_2F_4 - F_1F_3)}{F_2^2 - F_1^2}\delta_n^4 + P_3\frac{(F_2F_4 - F_1F_3)}{F_2^2 - F_1^2}\lambda_m^2\delta_n^2 - P_4\frac{(F_2F_3 - F_1F_4)}{F_2^2 - F_1^2}$$

$$-P_5\frac{(F_2F_3 - F_1F_4)}{F_2^2 - F_1^2} + P_6\lambda_m^4 + P_7\delta_n^4 + P_8\lambda_m^2\delta_n^2 - \frac{(F_2F_4 - F_1F_3)}{F_2^2 - F_1^2}\frac{\lambda_m^2}{R} - k_1 - k_2(\lambda_m^2 + \delta_n^2),$$

$$b_2 = h\left(P_x\lambda_m^2 + P_y\delta_n^2\right).$$

References

[1] Rango RF, Nallim LG, Oller S. Formulation of enriched macro elements using trigonometric shear deformation theory for free vibration analysis of symmetric laminated composite plate assemblies. Compos Struct 2015;119:38–49.

[2] Bodaghi M, Shakeri M, Aghdam MM. Thermo-mechanical behavior of shape adaptive composite plates with surface-bonded shape memory alloy ribbons. Compos Struct 2015;119:115–33.

[3] Sahoo R, Singh BN. A new trigonometric zigzag theory for buckling and free vibration analysis of laminated composite and sandwich plates. Compos Struct 2014;117:316–32.

[4] Samadpour M, Sadighi M, Shakeri M, Zamani HA. Vibration analysis of thermally buckled SMA hybrid composite sandwich plate. Compos Struct 2015;119:251–63.

[5] Moleiro F, Soares CMM, Soares CAM, Reddy JN. Layerwise mixed models for analysis of multilayered piezoelectric composite plates using least-squares formulation. Compos Struct 2015;119:134–49.

[6] Heydarpour Y, Aghdam MM, Malekzadeh P. Free vibration analysis of rotating functionally graded carbon nanotube-reinforced composite truncated conical shells. Compos Struct 2014;117:187–200.

[7] Lopatin AV, Morozov EV. Fundamental frequency of a cantilever composite cylindrical shell. Compos Struct 2015;119:638–47.

[8] Burgueño R, Hu N, Heeringa A, Lajnef N. Tailoring the elastic postbuckling response of thin-walled cylindrical composite shells under axial compression. Thin-Wall Struct 2014;84:14–25.

[9] Yang J, Xiong J, Ma L, Zhang G, Wang X, Wu L. Study on vibration damping of composite sandwich cylindrical shell with pyramidal truss-like cores. Compos Struct 2014;117:362–72.

[10] Vanin GA, Duc ND. The theory of spherofibrous composite.1: The input relations, hypothesis and models. Mech Compos Mater 1996;32(3):291-305.

[11] Shen MH, Chen FM, Hung SY. Piezoelectric study for a three-phase composite containing arbitrary inclusion. Int J Mech Sci 2010;52(4):561-71.

[12] Lin CB, Lee JL, Chen SC. Magnetoelastic stresses in a three-phase composite cylinder subject to a uniform magnetic induction. Int J Eng Sci 2010;48(5):529-49.

[13] Wu L, Pan S. Bounds on effective magnetic permeability of three-phase composites with coated spherical inclusions. Compos Sci Tech 2012;72(12):1443-50.

[14] Duc ND, Minh DK. Bending analysis of three-phase polymer composite plates reinforced by glass fibers and Titanium oxide particles. J Comput Mater Sci 2010;49(4):194-98.

[15] Afonso JC, Ranalli G. Elastic properties of three-phase composites: analytical model based on the modified shear-lag model and the method of cells. Compos Sci Tech 2005;65(7-8):1264-75.

[16] Andrianov IV, Danishevs'kyy VV, Kalamkarov AL. Asymptotic justification of the three-phase composite model. Compos Struct 2007:77(3):395-404.

[17] Duc ND, Quan TQ, Nam D. Nonlinear stability analysis of imperfect three phase polymer composite plates. Mech Compos Mater 2013;49(4):345-58.

[18] Duc ND, Thu PV. Nonlinear stability analysis of imperfect three-phase polymer composite plates in thermal environments. Compos Struct 2014;109:130-38.

[19] Volmir AS. Non-linear dynamics of plates and shells. Science Edition; 1972.

[20] Vanin GA. Micro-Mechanics of composite materials, "Nauka Dumka", Kiev; 1985.

[21] Matveev K. Hydrofoils and advanced marine vehicles; http://hydrofoils.org/.

[22] Thu PV, Quan TQ, Homayoun Hadavinia, Duc ND. Nonlinear dynamic analysis and vibration of imperfect three phase polymer nanocomposite panel resting on elastic foundation under hydrodynamic loads. Proceeding of the Third International Conference on Engineering Mechanics and Automation (ICEMA 3-2014, Hanoi,

October- 2014), 2014; 499-508.

[23] Thai HT, Kim SE. A review of theories for the modeling and analysis of functionally graded plates and shells. Composite Structures 2015;128:70-86.